

The object of this study is an 870 MW<sub>th</sub> small modular boiling water reactor (SMR-BWR) core that is expected to operate for 12 years without refueling. The main issue addressed is conventional BWR designs' limited fuel cycle duration, typically requiring refueling every 2–3 years. This short refueling period increases operational costs, leads to more extended maintenance downtimes, and generates larger volumes of spent fuel waste. This study examines the neutronic performance of thorium-based fuels, namely (Th-<sup>235</sup>U)O<sub>2</sub> and (Th-<sup>233</sup>U)O<sub>2</sub>, and compares them with standard UO<sub>2</sub> fuel in an SMR-BWR core configuration. The reactor core is a heterogeneous core consisting of 3 fuel zones. To control reactivity, a burnable poison in the form of B<sub>4</sub>C is also added to the fuel. Neutronic calculations are performed using the standard reactor analysis code (SRAC) system with the JENDL-4.0 nuclear data library. The SRAC code uses the PIJ module for fuel cell level calculations and the CITATION module for reactor core level calculations. The results show that (Th-<sup>233</sup>U)O<sub>2</sub> offers the most stable K<sub>eff</sub> over a 12-year operating period, consistently remaining above the criticality threshold at all fuel volume fractions. In addition, this fuel type exhibits the most uniform power density distribution and the lowest PPF values, reducing the potential for thermal hotspots. (Th-<sup>233</sup>U)O<sub>2</sub> fuel can achieve a burnup level of around 50,000 MWd/ton, which aligns with SMR-BWR standards. UO<sub>2</sub> and (Th-<sup>235</sup>U)O<sub>2</sub> fuels show a more pronounced K<sub>eff</sub> decrease and less favorable power distribution characteristics. These findings underline the potential of (Th-<sup>233</sup>U)O<sub>2</sub> as a promising candidate for long-cycle, continuous SMR-BWR applications without refueling.

**Keywords:** thorium fuel, extended fuel cycle, neutronic performance, <sup>233</sup>U, K<sub>eff</sub>, burnup level, power density distribution, PPF

# EVALUATION OF THORIUM-BASED FUELS FOR 12-YEAR OPERATION OF SMALL MODULAR BWR WITHOUT REFUELING

**Boni Pahlanop Lapanoro**

*Corresponding author*

Assistant Professor

Department of Physics, Faculty of Mathematics and Natural Sciences

Universitas Tanjungpura

Jl. Prof. Dr. H. Hadari Nawawi, Pontianak, Indonesia, 78124

E-mail: boni8poro@physics.untan.ac.id

**Zaki Su'ud**

Professor

Department of Physics, Faculty of Mathematics and Natural Sciences

Institut Teknologi Bandung

Jl. Ganesa 10, Bandung, Indonesia, 40132

Nuclear Physics & Biophysics Research Division

Institut Teknologi Bandung

Jl. Ganesa 10, Bandung, Indonesia, 40132

Received 05.05.2025

Received in revised form 01.06.2025

Accepted date 18.07.2025

Published date 28.08.2025.

**How to Cite:** Lapanoro, B. P., Su'ud, Z. (2025). Evaluation of thorium-based fuels for 12-year operation of small modular BWR without refueling.

*Eastern-European Journal of Enterprise Technologies*, 4 (5 (136)), 6–14.

<https://doi.org/10.15587/1729-4061.2025.335730>

## 1. Introduction

In response to global challenges related to clean energy transition and carbon emission reduction, developing safer, more efficient, and more sustainable nuclear energy systems has become a significant focus of contemporary energy research. One prominent approach gaining increasing attention in the nuclear reactors field is the deployment of small modular reactors (SMRs), which offer advantages such as standardized design, passive safety features, and adaptability for remote areas with limited infrastructure [1]. Among various SMR types, designs based on the boiling water reactor (BWR) are considered particularly promising due to their simplified cooling systems and the technological maturity of their core design. However, a critical limitation of BWR, including modular variants, is their relatively short fuel cycle, typically lasting only 2–3 years, necessitating frequent refueling. This constraint contributes to increased reactor downtime, elevated maintenance costs,

heightened safety risks, and the long-term accumulation of radioactive waste [2].

Developing fuel systems that enable long-term reactor operation without refueling is a critical issue in pursuing sustainable nuclear energy. Consequently, investigating alternative fuels capable of supporting extended fuel cycles has become increasingly important. Thorium-based fuels have attracted significant global attention due to the fertile nature thorium-232, which can be transmuted into fissile uranium-233 under neutron irradiation in the thermal spectrum. Thorium offers several advantages, including a high conversion ratio, reduced generation of minor actinides, and enhanced resistance to nuclear proliferation, positioning it as a strong candidate for long-cycle reactor applications [3].

Some studies have shown that researchers can optimize thorium-based fuel configurations to achieve stable neutronic performance and extend the reactor operating cycle [4]. However, the application of thorium in BWR systems remains a scientific challenge that requires further investigation, particularly

in the context of SMR designs, which demand both extended operational lifetimes and the maintenance of key neutronic parameters within strict safety margins. The study of thorium utilization in such systems remains highly relevant. It continues to garner significant scientific attention, driven by the increasing global demand for compact and inherently safe reactor technologies to support long-term energy security.

## 2. Literature review and problem statement

Thorium has been extensively studied as an alternative nuclear fuel for light water reactors (LWRs), including boiling water reactors (BWRs), due to its fertile characteristics that enable the production of fissile uranium-233 ( $^{233}\text{U}$ ) through neutron absorption in a thermal spectrum. Thorium offers several notable advantages compared to uranium, such as reduced generation of minor actinides and radiotoxic waste, higher conversion ratios, and enhanced resistance to nuclear proliferation. Furthermore, thorium is more abundant in the Earth's crust and exhibits strong potential for extending fuel cycle durations while minimizing long-term waste management challenges. As such, deploying thorium-based fuels represents a promising pathway for advancing the development of next-generation nuclear reactors with improved efficiency, sustainability, and safety performance [5].

Thorium ( $^{232}\text{Th}$ ) presents several advantages as a nuclear fuel, including its natural abundance four times greater than uranium, high conversion potential into fissile  $^{233}\text{U}$ , and reduced generation of long-lived radioactive waste. Moreover, thorium-based fuels offer the potential for incinerating  $^{239}\text{Pu}$ , thereby supporting nuclear non-proliferation objectives and contributing to cleaner energy production [6]. Despite these benefits, the deployment of thorium in BWR cores faces several technical and economic challenges. As  $^{232}\text{Th}$  is not fissile, it requires the addition of fissile isotopes such as  $^{235}\text{U}$ , typically enriched above 5%, which may increase fuel cycle costs. Furthermore, the presence of  $^{233}\text{Pa}$ , an intermediate product in the thorium fuel cycle, can elevate post-shutdown reactivity, while  $^{232}\text{U}$  complicates fuel handling and refabrication due to its intense gamma radiation [7]. These issues have limited the widespread adoption of thorium-based fuels in BWR systems. Addressing these challenges requires innovative design approaches, including optimizing fuel zone configurations, spectral control through core engineering, and integrating long-life modular reactor systems capable of maintaining neutronic safety margins throughout extended operational periods.

Various thorium fuel designs have been extensively explored using approaches such as blanket – seed configurations and axially heterogeneous assemblies. For instance, paper [8] evaluates multiple fuel assembly design options for BWRs operating in a closed and continuous  $\text{Th-}^{233}\text{U}$  fuel cycle. The proposed configuration employs an axially heterogeneous layout, with a single fissile zone positioned between two fertile blanket zones to enhance the fertility-to-fissile conversion ratio. The study identifies the optimal assembly parameters and zone dimensions to achieve net breeding of  $^{233}\text{U}$ . However, the investigation is limited to  $\text{Th-}^{233}\text{U}$  fuels and does not include comparisons with other fuel types, such as  $\text{UO}_2$  or  $\text{Th-}^{235}\text{U}$ . Similarly, paper [9] reports that using  $\text{UZr/ThO}_2$  composite fuel in BWRs can improve power density and fuel utilization efficiency relative to conventional  $\text{UO}_2$ . However, this study has not discussed the use of thorium-based fuel to extend the reactor operating cycle.

Comparative studies have examined the application of thorium in combination with various fissile materials, including  $^{235}\text{U}$ ,  $^{233}\text{U}$ , and  $^{239}\text{Pu}$ , within BWR systems. Paper [10] demonstrates that these configurations are technically feasible when implemented in the conventional GE-14N fuel assembly geometry, yielding neutronic safety parameters that are comparable to those of low-enriched uranium (LEU) and mixed oxide (MOX) fuels. Paper [11], which investigates the NuScale-type small modular reactor (SMR), reports that combining  $\text{ThO}_2$  with reprocessed fissile materials can significantly extend the fuel cycle beyond 25 MWd/kgHM and enhance the reactivity feedback coefficients. However, neither paper [10] nor paper [11] addresses the implementation of burnable poisons to manage long-term excess reactivity, which is essential for maintaining reactor safety over extended operating periods.

Previous studies have demonstrated the significant potential of thorium-based fuels for application in small modular reactors (SMRs), particularly in both homogeneous and heterogeneous core configurations. These fuel types have been shown to offer improved reactivity feedback coefficients and longer burnup cycles compared to conventional uranium-based fuels. However, the application of thorium fuels in small modular boiling water reactor (SMR-BWR) remains underexplored. Moreover, most prior studies have not addressed using burnable poisons to control long-term excess reactivity, an essential consideration for non-refueling fuel cycles. All this allows to assert that conducting a study on the neutronic feasibility of thorium-based fuels with integrated burnable poisons in SMR-BWRs for long-cycle, non-refueling operation is expedient.

## 3. The aim and objectives of the study

The aim of this study is to identify features of three different fuel configurations  $\text{UO}_2$ ,  $(\text{Th-}^{235}\text{U})\text{O}_2$ , and  $(\text{Th-}^{233}\text{U})\text{O}_2$  within the core design of an 870 MW<sub>th</sub> SMR-BWR, in order to assess the potential of thorium-based fuels to extend the operational cycle up to 12 years without refueling, without compromising safety margins or the stability of power distribution within the reactor core.

To achieve this aim, the following objectives were accomplished:

- to determine the fuel configuration that maintains the most stable effective multiplication factor ( $K_{eff}$ ) over a 12-year operation period;
- to analyze radial and axial power density distributions to evaluate the stability of power generation;
- to calculate the power peaking factor (PPF) as an indicator of power uniformity and hotspot potential;
- to assess the fuel burnup level as an indicator of fissile material utilization efficiency during long-cycle operation.

## 4. Materials and methods

The object of this study is an SMR-BWR with a thermal power of 870 MW<sub>th</sub>. It is designed to operate for 12 years without refueling. The central hypothesis of this study is that thorium-based fuels, particularly  $(\text{Th-}^{233}\text{U})\text{O}_2$ , can maintain reactivity above criticality for 12 years with acceptable power distribution and burnup levels in an SMR-BWR core. Key assumptions include constant geometry across all cases and the homogeneous mixing of burnable poisons. The primary simplification uses a two-dimensional (2D R-Z) model without thermal-hydraulic coupling.

The present study conducts a comparative neutronic evaluation of three fuel types  $\text{UO}_2$ ,  $(\text{Th}^{235}\text{U})\text{O}_2$ , and  $(\text{Th}^{233}\text{U})\text{O}_2$  within the core configuration of an 870 MW<sub>th</sub> SMR-BWR. The analysis focuses on key neutronic parameters, including the effective multiplication factor ( $K_{eff}$ ), power density distribution, power peaking factor (PPF), and burnup level, to assess reactivity stability, fuel utilization efficiency, and operational safety. By incorporating  $\text{B}_4\text{C}$  as a standard burnable poison, this study proposes a viable strategy to maintain low excess reactivity over a 12-year operating period without refueling while preserving safety margins and ensuring uniform power distribution.

The fuel cell model uses a square cell geometry, as shown in Fig. 1. The pitch (distance between fuel rod centers) is 1.45 cm. Each cell consists of a cylindrical fuel pellet clad with Zircaloy-4 and surrounded by light water ( $\text{H}_2\text{O}$ ) as a moderator. The fuel volume fractions analyzed in this study are 55%, 60%, and 65%. In this study, let's vary the fuel volume fraction by adjusting the fuel pellet diameter while maintaining a constant fuel pin pitch. This parametric variation was performed to analyze how neutronic performance responds to different fuel-to-moderator ratios, making it an essential part of evaluating the impact of fuel volume fraction on key neutronic parameters.

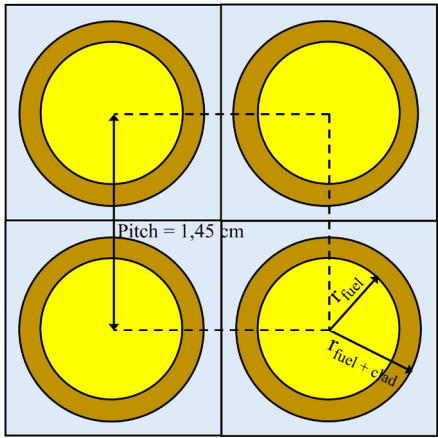


Fig. 1. Fuel cell configuration

To control the initial excess reactivity and maintain reactor stability throughout the cycle, burnable poison (BP) in boron carbide ( $\text{B}_4\text{C}$ ) is used, homogeneously mixed with the fuel.  $\text{B}_4\text{C}$  is chosen due to its high thermal neutron absorption capability and good chemical stability under light water reactor conditions. It is acknowledged that the use of  $\text{B}_4\text{C}$  as an integral burnable poison (IBP) by homogeneous mixing with fuel is not standard in current BWR practice. This study adopts  $\text{B}_4\text{C}$  as a conceptual IBP to evaluate its neutronic effect. While technologically feasible, practical implementation would require addressing manufacturing challenges, such as differences in thermal expansion coefficients, sintering compatibility, and achieving homogeneous distribution within the fuel matrix.

The reactor core is modeled as a cylinder with a height of 313.2 cm and a diameter of 130.5 cm. An R-Z geometry approximation is used for two-dimensional calculations, in which the core is divided into three fuel zones (A, B, and C) with different levels of fissile enrichment. Zone A represents the region with the lowest enrichment, Zone B has medium enrichment, and Zone C has the highest enrichment level. The distribution of these fuel zones is arranged radially, as illustrated in Fig. 2,

with a reflector placed around the outer boundary of the core to enhance neutron utilization and fuel burnup efficiency [12]. The fissile material enrichment settings for each zone for the three fuel types analyzed are presented in Table 1. It is determined that the fuel enrichment based on the requirement to achieve adequate initial reactivity while remaining within the safety design limits of the SMR-BWR. The enrichment values of 4.5–6.5% for  $^{235}\text{U}$  and  $^{233}\text{U}$  were chosen considering results from our previous parametric studies to ensure criticality and safety throughout the 12-year operation [1].

Table 1

Fissile material enrichment in each core zone for each fuel type

| Fuel type                             | Zone A (lowest enrichment) | Zone B (medium enrichment) | Zone C (highest enrichment) |
|---------------------------------------|----------------------------|----------------------------|-----------------------------|
| $\text{UO}_2$                         | 4.5% $^{235}\text{U}$      | 5% $^{235}\text{U}$        | 5.5% $^{235}\text{U}$       |
| $(\text{Th}^{235}\text{U})\text{O}_2$ | 5.5% $^{235}\text{U}$      | 6% $^{235}\text{U}$        | 6.5% $^{235}\text{U}$       |
| $(\text{Th}^{233}\text{U})\text{O}_2$ | 4.5% $^{233}\text{U}$      | 5% $^{233}\text{U}$        | 5.5% $^{233}\text{U}$       |

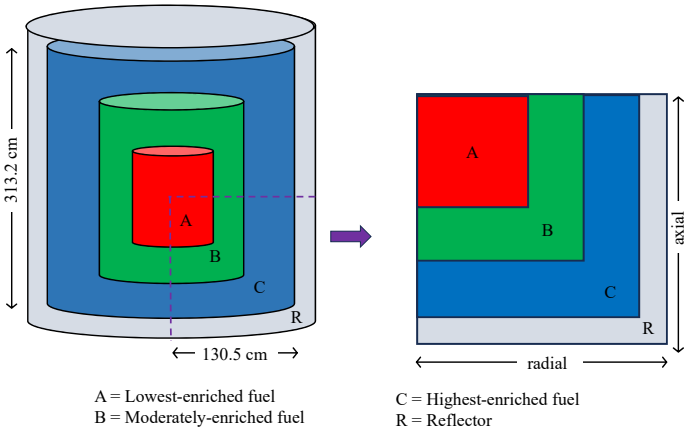


Fig. 2. Reactor core configuration

Several key neutronic parameters calculated in this study include the effective multiplication factor ( $K_{eff}$ ) over 12 years of operation as an indicator of reactivity sustainability, radial and axial power density distributions to assess the uniformity of power generation, and the power peaking factor (PPF) as a measure of power distribution stability. In addition, the fuel burnup level was calculated to evaluate the efficiency of fissile material utilization, where a higher burnup reflects more optimal fuel use. These parameters were analyzed for each fuel type to assess neutronic stability and feasibility within a long-life, safe, and efficient SMR-BWR core design. The SMR-BWR design parameters are presented in Table 2. It is possible to refer to the power level of 870 MW<sub>th</sub> based on the BWRX-300, an SMR-BWR developed by Hitachi. In this study, it is possible to design the reactor core to ensure that the average power density remains close to the standard values used in conventional BWR [13].

Neutronic calculations were performed using the standard reactor analysis code (SRAC) 2006 version, utilizing the PIJ module for fuel cell-level calculations and the CITATION module for core-level flux and reactivity distribution analysis. This study used nuclear data obtained from the JENDL-4.0 library. The calculation scheme is illustrated in Fig. 3 [14].

Table 2

Small modular BWR design parameters

| Parameters  | Specification   |
|---|---|
| Thermal power reactors (MW <sub>th</sub> )          | 870   |
| Fuel  | UO <sub>2</sub> , (Th- <sup>235</sup> U)O <sub>2</sub> , and (Th- <sup>233</sup> U)O <sub>2</sub> |
| Cladding structure                                  | Zircaloy-4  |
| Coolant   | H <sub>2</sub> O  |
| Reflector   | Stainless steel and H <sub>2</sub> O  |
| Fuel cell geometry                                  | Square cell   |
| <sup>235</sup> U or <sup>233</sup> U percentage (%) | 4.5–6.5   |
| Fuel volume fraction (%)                            | 55, 60, and 65  |
| Cladding density (g/cm <sup>3</sup> )               | 6.5   |
| Cladding thickness (cm)                             | 0.057   |
| Coolant density (g/cm <sup>3</sup> )                | 0.72  |
| Pin pitch (cm)                                      | 1.45 cm   |
| Active core diameter (cm)                           | 261.0 cm  |
| Active core height (cm)                             | 313.2 cm  |

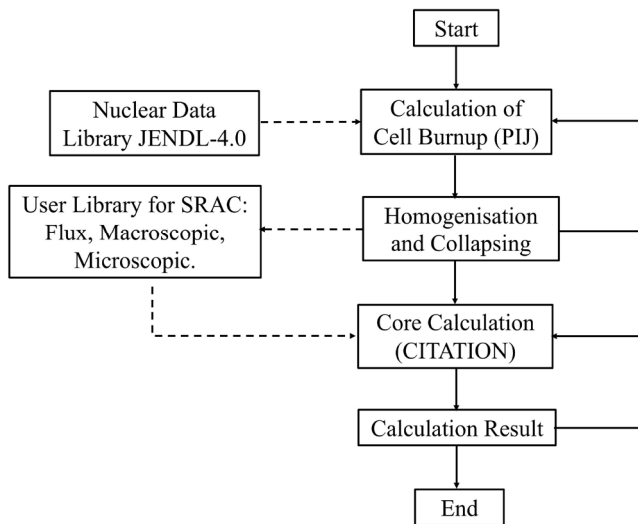


Fig. 3. Calculation scheme of standard reactor analysis code

The diagram in Fig. 3 illustrates the calculation flow from the fuel cell data processing stage to the core-level neutronic distribution, which is the basis for evaluating the reactor performance parameters in this study.

## 5. Results of evaluation of thorium-based fuels for 12-year operation of small modular BWR without refueling

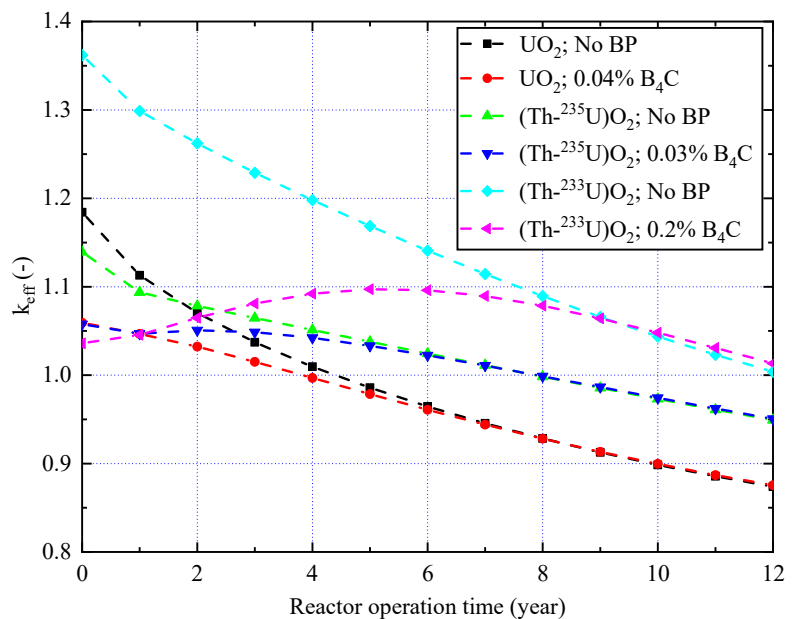
### 5.1. Effective multiplication factor ( $K_{eff}$ )

The effective multiplication factor ( $K_{eff}$ ) was calculated for three fuel volume fraction scenarios, 55%, 60%, and 65%, to evaluate the impact of fuel volume fraction on the reactor's neutronic performance. This study tested each configuration for all three fuel types UO<sub>2</sub>, (Th-<sup>235</sup>U)O<sub>2</sub>, and (Th-<sup>233</sup>U)O<sub>2</sub> with and without burnable poison (B<sub>4</sub>C), to analyze reactivity trends over a 12-year operation and determine the most stable neutronic configuration.

Fig. 4 shows the effective multiplication factor ( $K_{eff}$ ) profiles over 12 years of operation for the three fuel types UO<sub>2</sub>, (Th-<sup>235</sup>U)O<sub>2</sub>, and (Th-<sup>233</sup>U)O<sub>2</sub> with and without the use of burnable poison (B<sub>4</sub>C), at a fuel volume fraction of 55%. The UO<sub>2</sub> fuel without BP exhibits a high initial  $K_{eff}$  (~1.31) but drops significantly to subcritical levels (<1.0) by years 5 to 6. The addition of 0.04% B<sub>4</sub>C reduces the initial reactivity but is insufficient to maintain criticality throughout the 12 years. Meanwhile, (Th-<sup>235</sup>U)O<sub>2</sub> shows a more moderate initial  $K_{eff}$  and a slower decline, with 0.03% B<sub>4</sub>C helping to smooth the reactivity decrease, although  $K_{eff}$  still falls below one by the end of the cycle. The (Th-<sup>233</sup>U)O<sub>2</sub> fuel demonstrates the best performance, starting with a high  $K_{eff}$  (~1.36) and declining very slowly, remaining critical through the end of the operation. 0.2% B<sub>4</sub>C lowers the initial  $K_{eff}$  to ~1.06 but maintains a value above 1 for nearly the entire operation period, indicating excellent neutronic stability and the highest potential for long-life reactor applications.

As shown in Fig. 5, at a fuel volume fraction of 60%, the increased fissile nuclide density results in a higher initial  $K_{eff}$  than the 55% fraction. However, a decrease in  $K_{eff}$  still occurs, particularly for UO<sub>2</sub> and (Th-<sup>235</sup>U)O<sub>2</sub>, which become subcritical from year 5 to 6, regardless of the presence of B<sub>4</sub>C. This result indicates that increasing the fuel volume fraction alone is insufficient for long-term reactivity. In contrast, (Th-<sup>233</sup>U)O<sub>2</sub> shows the best performance: without BP, it starts with a high  $K_{eff}$  (~1.32) and remains critical until the end of the operation; with 0.2% B<sub>4</sub>C, the initial reactivity drops to ~1.05 but remains stable and close to 1.00 throughout the 12 years. (Th-<sup>235</sup>U)O<sub>2</sub> exhibits intermediate performance with moderate initial reactivity and a slow decline but remains subcritical by the end of the cycle, making it suitable for thorium transition cycles, although less optimal compared to (Th-<sup>233</sup>U)O<sub>2</sub>.

Fig. 6 presents the effective multiplication factor ( $K_{eff}$ ) profiles for small modular BWRs operating with a fuel volume fraction of 65%. The profiles correspond to three fuel types: UO<sub>2</sub>, (Th-<sup>233</sup>U)O<sub>2</sub>, and (Th-<sup>235</sup>U)O<sub>2</sub>.

Fig. 4. Effective multiplication factor ( $K_{eff}$ ) profile for a small modular BWR with a fuel volume fraction of 55% using the three fuel types



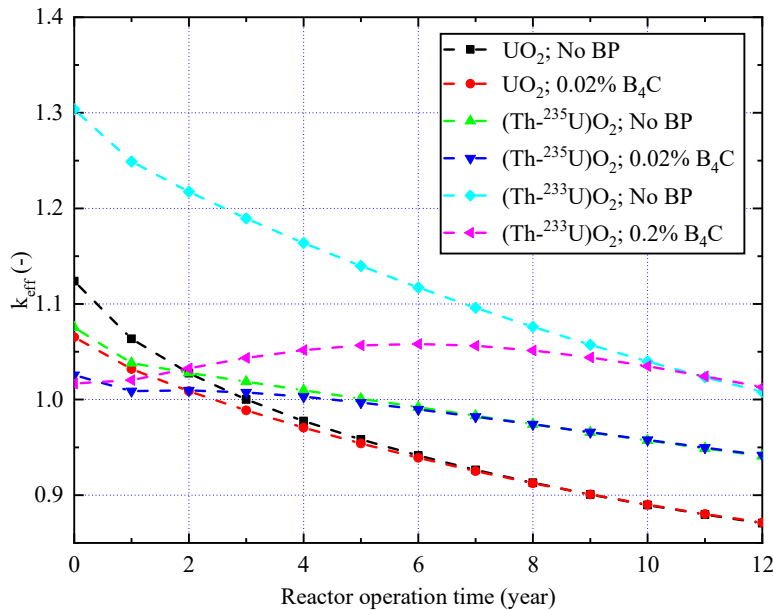


Fig. 5. Effective multiplication factor ( $K_{eff}$ ) profile for a small modular BWR with a fuel volume fraction of 60% using the three fuel types

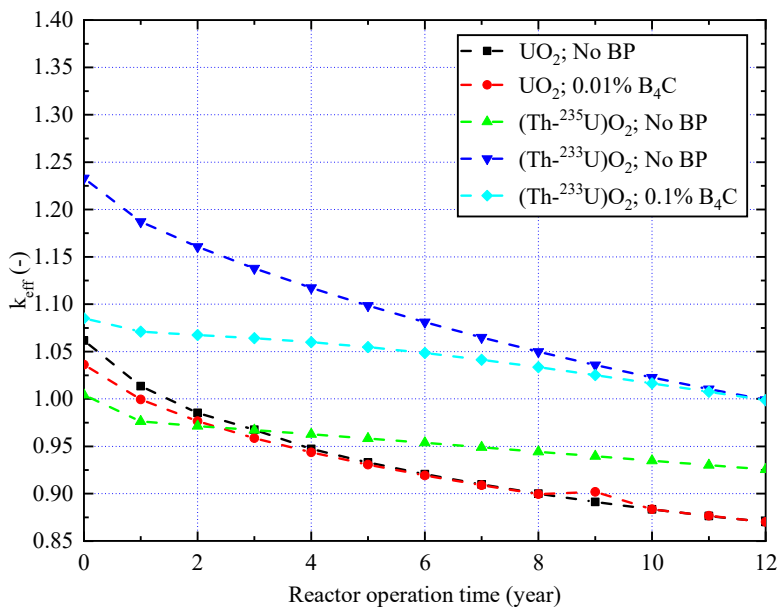


Fig. 6. Effective multiplication factor ( $K_{eff}$ ) profile for a small modular BWR with a fuel volume fraction of 65% using the three fuel types

Fig. 6 shows that at a fuel volume fraction of 65%, the increase in fissile density has varying impacts depending on the fuel type.  $(\text{Th-}^{233}\text{U})\text{O}_2$  demonstrates the best performance, with a high initial  $K_{eff}$  (~1.23) without BP, and remains critical throughout the 12 years. Adding 0.1%  $\text{B}_4\text{C}$  reduces the initial  $K_{eff}$  to ~1.08 but maintains stability over the entire cycle, reflecting the high fissility of  $^{233}\text{U}$  and its responsiveness to burnable poison. In contrast,  $\text{UO}_2$  experiences a rapid drop in  $K_{eff}$  despite an initial value of ~1.06; adding 0.01%  $\text{B}_4\text{C}$  only slightly improves the initial reactivity. Surprisingly,  $(\text{Th-}^{235}\text{U})\text{O}_2$  exhibits an initial  $K_{eff}$  below 1, indicating a subcritical condition from the start and a lack of sustainability without a more complex reactor design.

## 5. 2. Power density distribution

The power density distribution was obtained from the small modular BWR core calculations using the CITATION module of the SRAC program. In this section, the presented power distribution corresponds to the fuel volume fraction of 60% with the addition of  $\text{B}_4\text{C}$  as a burnable poison (BP). The distribution is shown for both radial and axial directions at the beginning of the cycle (BOC) and end of the cycle (EOC) for the three fuel types:  $\text{UO}_2$ ,  $(\text{Th-}^{235}\text{U})\text{O}_2$ , and  $(\text{Th-}^{233}\text{U})\text{O}_2$ . The radial distributions were taken at the core mid-plane ( $z = 156.6$  cm). In comparison, the axial distributions were taken at the core centerline ( $r = 0$  cm), with central power density values highlighted for reference.

Radial and axial power distributions for  $\text{UO}_2$  fuel are presented in Fig. 7. The results reflect the configuration with 0.02%  $\text{B}_4\text{C}$  added as a burnable poison.

The power density distribution for  $\text{UO}_2$  fuel exhibits typical patterns both radially and axially. Radially, as shown in Fig. 7, a, at the BOC, the maximum power (~82 W/cc) is concentrated at the core center and decreases toward the periphery, reflecting the neutron flux peak at the center. The overall distribution weakens toward the EOC, with the peak power decreasing to ~60 W/cc due to reduced reactivity. As shown in Fig. 7, b, the initial distribution is uniform in the axial direction from the bottom to the mid-height (~40–45 W/cc), then increases toward the top. By the EOC, the power peak shifts upward, reaching ~62 W/cc, indicating a shift in reactivity location due to fuel burnup.

Radial and axial power distributions for  $(\text{Th-}^{235}\text{U})\text{O}_2$  fuel are presented in Fig. 8. The results reflect the configuration with 0.02%  $\text{B}_4\text{C}$  added as a burnable poison.

The power density distribution of  $(\text{Th-}^{235}\text{U})\text{O}_2$  fuel shows significant changes between the BOC and EOC. As illustrated in Fig. 8, a, the radial distribution at BOC is relatively uniform in the core center with a peak of ~55 W/cc but increases sharply at EOC to ~95 W/cc at the center. This result reflects reactivity buildup due to thorium conversion into  $^{233}\text{U}$ . Meanwhile, Fig. 8, b shows that the axial distribution at BOC is relatively uniform (48–52 W/cc) and,

at EOC, increases slightly with a peak of ~57 W/cc at the upper core region. Overall, the axial distribution remains stable, but the radial peaking at EOC should be considered in thermal design to avoid overheating.

Radial and axial power distributions for  $(\text{Th-}^{233}\text{U})\text{O}_2$  fuel are presented in Fig. 9. The results reflect the configuration with 0.02%  $\text{B}_4\text{C}$  added as a burnable poison.

The power density distribution of  $(\text{Th-}^{233}\text{U})\text{O}_2$  fuel demonstrates superior characteristics to the other two fuels. As shown in Fig. 9, a, the radial power distribution at BOC is relatively moderate (~50 W/cc) at the core center and decreases toward the periphery. At EOC, the power increases significantly at the center to ~85 W/cc due to  $^{233}\text{U}$  buildup, resulting in a steeper profile. Meanwhile, Fig. 9, b indicates

that the axial power distribution at BOC tends to rise from bottom to top, peaking at  $\sim 51$  W/cc. At EOC, the distribution becomes more uniform ( $\sim 48$ – $50$  W/cc), indicating vertical

power stability. Overall,  $(\text{Th-}^{233}\text{U})\text{O}_2$  offers advantages in axial stability and radial reactivity efficiency, with special attention required for core-center peaking at the end of the cycle.

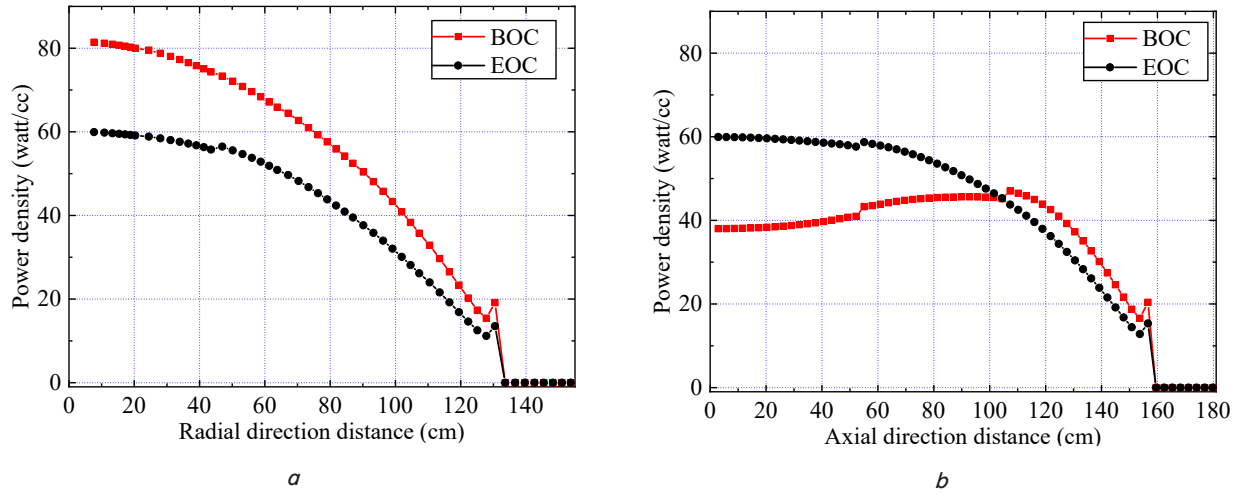


Fig. 7. Power density distribution for  $\text{UO}_2$  fuel with 0.02%  $\text{B}_4\text{C}$  and a fuel volume fraction of 60%;  $a$  – radial direction;  $b$  – axial direction (1 mesh = 2.90 cm)

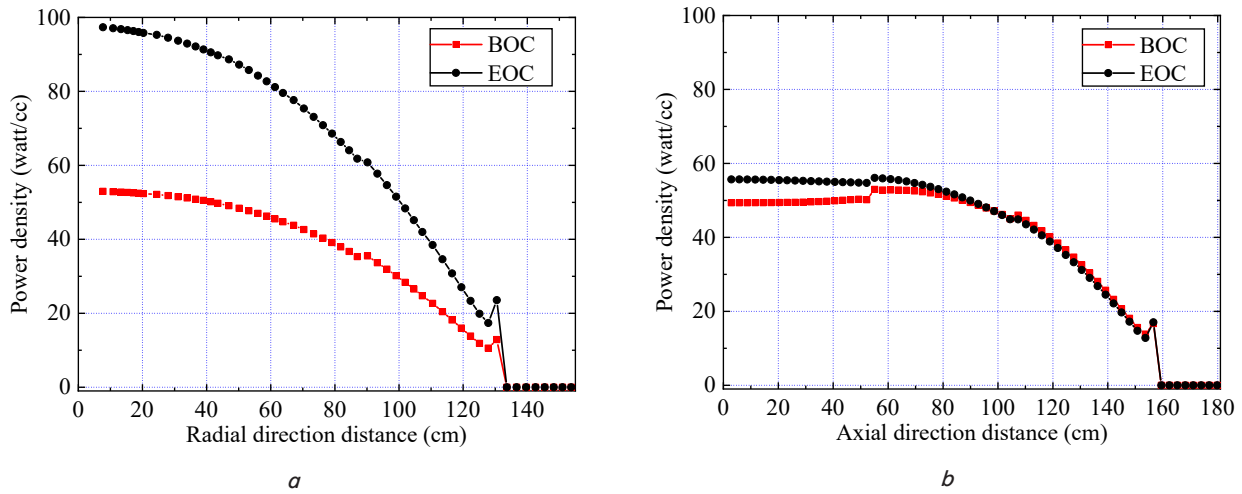


Fig. 8. Power density distribution for  $(\text{Th-}^{235}\text{U})\text{O}_2$  fuel with 0.02%  $\text{B}_4\text{C}$  and a fuel volume fraction of 60%;  $a$  – radial direction;  $b$  – axial direction (1 mesh = 2.90 cm)

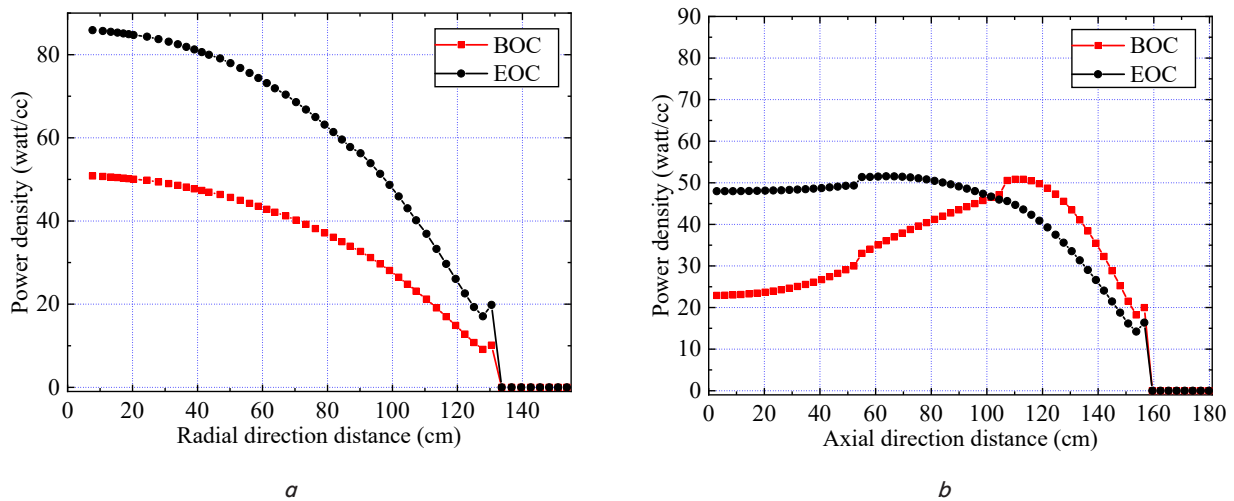


Fig. 9. Power density distribution for  $(\text{Th-}^{233}\text{U})\text{O}_2$  fuel with 0.2%  $\text{B}_4\text{C}$  and a fuel volume fraction of 60%;  $a$  – radial direction;  $b$  – axial direction (1 mesh = 2.90 cm)

### 5.3. Power peaking factor

Table 3 presents the power peaking factor (PPF) values in both radial and axial directions at the beginning of cycle (BOC) and end of cycle (EOC) for different fuel types  $\text{UO}_2$ ,  $(\text{Th}^{235}\text{U})\text{O}_2$ , and  $(\text{Th}^{233}\text{U})\text{O}_2$  under varying fuel volume fractions (%Fuel) of 55%, 60%, and 65%, and different burnable poison ( $\text{B}_4\text{C}$ ) concentrations. Generally, radial PPF values at BOC tend to be higher than at EOC, indicating a reduction in initial power peaking as fissile material is consumed.  $\text{UO}_2$  fuel exhibits the highest radial PPF at BOC (up to 1.79), which decreases at EOC but remains relatively high. The use of  $\text{B}_4\text{C}$  has been shown to reduce PPF values, as seen in  $\text{UO}_2$  with 55% fuel and 0.04%  $\text{B}_4\text{C}$ , where the radial PPF at BOC decreased from 1.79 to 1.67.

For  $(\text{Th}^{235}\text{U})\text{O}_2$  fuel, the radial and axial PPF values are generally lower and more stable, indicating a more uniform power profile. Meanwhile,  $(\text{Th}^{233}\text{U})\text{O}_2$  shows good axial power stability, with axial PPF values ranging from 1.19 to 1.22. However, a significant radial PPF increase is observed when  $\text{B}_4\text{C}$  is used. For example, at a 65% fuel fraction with 0.10%  $\text{B}_4\text{C}$ , the axial PPF reaches 1.36.

Table 3

PPF values for each fuel type and volume fraction

| Fuel                                  | %Fuel | %B <sub>4</sub> C | BOC    |       | EOC    |       |
|---------------------------------------|-------|-------------------|--------|-------|--------|-------|
|                                       |       |                   | Radial | Axial | Radial | Axial |
| $\text{UO}_2$                         | 55    | 0.00              | 1.79   | 1.26  | 1.72   | 1.22  |
| $\text{UO}_2$                         | 55    | 0.04              | 1.67   | 1.20  | 1.72   | 1.23  |
| $\text{UO}_2$                         | 60    | 0.00              | 1.75   | 1.25  | 1.73   | 1.23  |
| $\text{UO}_2$                         | 60    | 0.02              | 1.66   | 1.22  | 1.74   | 1.23  |
| $\text{UO}_2$                         | 65    | 0.00              | 1.71   | 1.24  | 1.65   | 1.25  |
| $\text{UO}_2$                         | 65    | 0.01              | 1.67   | 1.22  | 1.75   | 1.23  |
| $(\text{Th}^{235}\text{U})\text{O}_2$ | 55    | 0.00              | 1.60   | 1.15  | 1.67   | 1.26  |
| $(\text{Th}^{235}\text{U})\text{O}_2$ | 55    | 0.03              | 1.73   | 1.20  | 1.67   | 1.26  |
| $(\text{Th}^{235}\text{U})\text{O}_2$ | 60    | 0.00              | 1.75   | 1.15  | 1.70   | 1.27  |
| $(\text{Th}^{235}\text{U})\text{O}_2$ | 60    | 0.02              | 1.73   | 1.19  | 1.70   | 1.27  |
| $(\text{Th}^{235}\text{U})\text{O}_2$ | 65    | 0.00              | 1.73   | 1.19  | 1.70   | 1.27  |
| $(\text{Th}^{233}\text{U})\text{O}_2$ | 55    | 0.00              | 1.74   | 1.21  | 1.66   | 1.19  |
| $(\text{Th}^{233}\text{U})\text{O}_2$ | 55    | 0.20              | 1.69   | 1.48  | 1.66   | 1.20  |
| $(\text{Th}^{233}\text{U})\text{O}_2$ | 60    | 0.00              | 1.74   | 1.22  | 1.65   | 1.19  |
| $(\text{Th}^{233}\text{U})\text{O}_2$ | 60    | 0.20              | 1.70   | 1.46  | 1.67   | 1.19  |
| $(\text{Th}^{233}\text{U})\text{O}_2$ | 65    | 0.00              | 1.73   | 1.23  | 1.65   | 1.19  |
| $(\text{Th}^{233}\text{U})\text{O}_2$ | 65    | 0.10              | 1.68   | 1.36  | 1.67   | 1.19  |

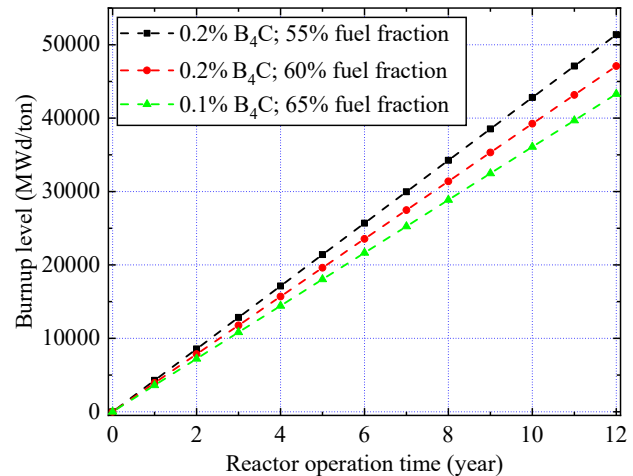
From Table 3, it can be concluded that  $(\text{Th}^{233}\text{U})\text{O}_2$  fuel tends to provide a more uniform axial power distribution, while  $\text{UO}_2$  exhibits higher power peaking and is more sensitive to variations in fuel volume fraction and  $\text{B}_4\text{C}$  usage. This information is crucial for thermal analysis and the long-term safety design of the reactor core.

### 5.4. Burnup level

Fig. 10 illustrates the relationship between reactor operating time (in years) and burnup level (in MWd/ton) for  $(\text{Th}^{233}\text{U})\text{O}_2$ , with fuel volume fractions of 55%, 60%, and 65%, respectively, with  $\text{B}_4\text{C}$  additions to each fuel volume fraction of 0.2%, 0.2%, and 0.1%. In general, the addition of  $\text{B}_4\text{C}$  does not have a significant effect on the burnup level because the percentage is tiny.

At the end of the reactor operating cycle for 12 years, it can be seen that the burnup rate can reach 51,373 MWd/ton at a fuel fraction of 55%, 47,092 MWd/ton at a fuel volume

fraction of 60%, and 43,296 MWd/ton at a fuel volume fraction of 65%. It can be seen that the burnup rate is higher at a lower fuel volume fraction. This condition occurs because the lower fuel volume fraction means a larger moderator, so the thermal neutrons increase, causing fuel burnup to increase.

Fig. 10. Burnup level for  $(\text{Th}^{233}\text{U})\text{O}_2$  fuel with variations in fuel volume fraction

## 6. Discussion of evaluation of thorium-based fuels for 12-year operation of small modular BWR without refueling

The evaluation of thorium-based fuels for 12-year operation of small modular BWR without refueling was conducted using four main neutronic parameters: the effective multiplication factor ( $K_{eff}$ ), power density distribution, Power Peaking Factor (PPF), and burnup level.

The  $K_{eff}$  results are presented in Fig. 4–6 show that  $(\text{Th}^{233}\text{U})\text{O}_2$  fuel provides the most stable reactivity performance over 12 years. Without burnable poison (BP), its initial  $K_{eff}$  reaches  $\sim 1.36$  (Fig. 4), indicating high excess reactivity. The addition of 0.2%  $\text{B}_4\text{C}$  successfully reduces this to  $\sim 1.06$ , maintaining criticality throughout the cycle. The in-situ breeding of  $^{233}\text{U}$  from  $^{232}\text{Th}$  contributes significantly to sustaining reactivity, making this configuration ideal for long-life core applications.

In contrast,  $\text{UO}_2$  fuel demonstrates a steep decline in  $K_{eff}$  and becomes subcritical after 5–6 years regardless of  $\text{B}_4\text{C}$  addition, as seen in Fig. 4, 5. Although  $(\text{Th}^{235}\text{U})\text{O}_2$  performs better with slower  $K_{eff}$  reduction, it still falls below critical by the end of 12 years. This result confirms that thorium fuel with  $^{233}\text{U}$  provides superior long-term reactivity, which aligns with results from earlier works [4, 5].

Fig. 7–9 illustrate the radial and axial power density distributions at BOC and EOC for the three fuel types. For  $\text{UO}_2$  (Fig. 7), the peak radial power density is  $\sim 82$  W/cc at BOC, decreasing to  $\sim 60$  W/cc at EOC. In the axial direction, the power peak shifts upward by EOC, suggesting reactivity migration, which must be considered in thermal-hydraulic design. For  $(\text{Th}^{235}\text{U})\text{O}_2$  (Fig. 8), the radial distribution becomes increasingly peaked, rising to  $\sim 95$  W/cc at EOC due to localized  $^{233}\text{U}$  buildup. The axial profile remains relatively stable. In contrast,  $(\text{Th}^{233}\text{U})\text{O}_2$  (Fig. 9) shows symmetric radial peaking from  $\sim 50$  to  $\sim 85$  W/cc and a consistent axial profile ( $\sim 48$ – $50$  W/cc), indicating well-balanced reactivity and thermal behavior.

Table 3 provides PPF data, which further supports these observations.  $\text{UO}_2$  exhibits the highest PPF values, especially radially.  $(\text{Th}^{235}\text{U})\text{O}_2$  shows significant radial peaking at EOC, while  $(\text{Th}^{233}\text{U})\text{O}_2$  maintains the lowest and most stable PPFs in both directions, indicating better power flattening.

The burnup level in Fig. 10 shows that the  $(\text{Th}^{233}\text{U})\text{O}_2$  fuel can achieve a burnup level of 51,373 MWd/ton at a fuel fraction of 55%, 47,092 MWd/ton at a fuel volume fraction of 60%, and 43,296 MWd/ton at a fuel volume fraction of 65% at the end of the operating cycle. These results are close to the standard SMR-BWR type BWRX-300, which has a projected burnup level of up to 50,000 MWd/ton [13].

Compared to prior research, this study provides a detailed, fuel-to-fuel evaluation under consistent 870 MW<sub>th</sub> small modular BWR conditions with design-specific power densities and long-life cycle aims. The results align with earlier findings [6, 10, 11, 15] while introducing new data on reactor-scale distribution behavior and long-term reactivity control at that power level.

In conclusion, based on all evaluated parameters,  $(\text{Th}^{233}\text{U})\text{O}_2$  emerges as the most viable fuel candidate for enabling up to 12 years of continuous operation in small modular BWRs without refueling, offering substantial advantages in reactivity stability, power distribution uniformity, and fissile material utilization.

However, this study has several limitations, including using a two-dimensional (2D R-Z) core geometry model that does not describe the power density distribution in all directions in the reactor core. In addition, neutronic calculations were performed without thermal-hydraulic analysis, so the effects of temperature and fuel cooling have not been calculated realistically. Therefore, further development must include three-dimensional (3D) modeling, neutronic and thermal-hydraulic integration analysis, and transient safety evaluation to ensure comprehensive reactor design performance and satisfaction.

In addition to the technical limitations of the two-dimensional core model and the absence of thermal-hydraulic coupling, this study also presents several notable shortcomings. A key drawback is the exclusive reliance on simulation-based analysis, which has not yet been experimentally validated or benchmarked against real reactor data. This lack of validation may result in discrepancies when the results are applied to more complex physical conditions. To address this issue, future work should include benchmarking simulation outcomes using experimental data or well-established reactor benchmarks to improve result reliability.

Future development of this study should focus on extending the current methodology to complete three-dimensional modeling with integrated neutronic and thermal-hydraulic coupling. In addition, transient and accident condition analyses are necessary to ensure comprehensive safety evalua-

tion. However, such developments are expected to encounter several challenges, including the need for significant computational resources to perform long-term 3D simulations and the use of advanced multiphysics codes capable of modeling detailed thermal-hydraulic behavior under operational and off-normal conditions.

7. Conclusions

1. The  $(\text{Th}^{233}\text{U})\text{O}_2$  fuel exhibits the most stable  $K_{eff}$  values, consistently remaining above 1.00 throughout 12 years of operation without refueling, making it a strong candidate for long-cycle applications. Adding burnable poison ( $\text{B}_4\text{C}$ ) has reduced the initial excess reactivity.
2.  $(\text{Th}^{233}\text{U})\text{O}_2$  exhibits a symmetric radial power distribution with a moderate increase at the core center by the end of the cycle, reflecting efficient reactivity utilization and optimal power control. Its axial power distribution also remains stable throughout the operational cycle, contributing to thermal stability within the reactor.
3. The power peaking factor (PPF) values for  $(\text{Th}^{233}\text{U})\text{O}_2$  fuel tend to remain lower and more stable throughout the cycle, with radial PPF values for all fuel volume fractions ranging from 1.65 to 1.74 and axial PPF from 1.19 to 1.48, indicating a uniform power distribution and minimal risk of hotspot formation.
4.  $(\text{Th}^{233}\text{U})\text{O}_2$  fuel can achieve a burnup level of around 50,000 MWd/ton, which aligns with SMR-BWR standards.

Conflict of interest

The authors declare that they have no conflict of interest in relation to this study, whether financial, personal, authorship or otherwise, that could affect the study and its results presented in this paper.

Financing

The study was performed without financial support.

Data availability

Manuscript has no associated data.

Use of artificial intelligence

The authors confirm that they did not use artificial intelligence technologies when creating the current work.

References

1. Lapanporo, B. P., Su'ud, Z. (2022). Parametric Study of Thorium Fuel Utilization on Small Modular Pressurized Water Reactors (PWR). *Journal of Physics: Conference Series*, 2243 (1), 012062. <https://doi.org/10.1088/1742-6596/2243/1/012062>

2. Science, N. (2013). Minor Actinide Burning in Thermal Reactors A Report. Working Party. Nuclear Energy Agency.

3. Humphrey, U. E., Khandaker, M. U. (2018). Viability of thorium-based nuclear fuel cycle for the next generation nuclear reactor: Issues and prospects. *Renewable and Sustainable Energy Reviews*, 97, 259–275. <https://doi.org/10.1016/j.rser.2018.08.019>

4. Du Toit, M. H., Van Niekerk, F., Amirkhosravi, S. (2024). Review of thorium-containing fuels in LWRs. *Progress in Nuclear Energy*, 170, 105136. <https://doi.org/10.1016/j.pnucene.2024.105136>



5. Galahom, A. A., Mohsen, M. Y. M., Amrani, N. (2022). Explore the possible advantages of using thorium-based fuel in a pressurized water reactor (PWR) Part 1: Neutronic analysis. *Nuclear Engineering and Technology*, 54 (1), 1–10. <https://doi.org/10.1016/j.net.2021.07.019>
6. Lobo, M. C. A., Stefani, G. L. de. (2024). Thorium as nuclear fuel in Brazil: 1951 to 2023. *Nuclear Engineering and Design*, 419, 112912. <https://doi.org/10.1016/j.nucengdes.2024.112912>
7. Gorton, J. P., Collins, B. S., Nelson, A. T., Brown, N. R. (2019). Reactor performance and safety characteristics of ThN-UN fuel concepts in a PWR. *Nuclear Engineering and Design*, 355, 110317. <https://doi.org/10.1016/j.nucengdes.2019.110317>
8. Shaposhnik, Y., Shwageraus, E., Elias, E. (2013). Core design options for high conversion BWRs operating in Th-<sup>233</sup>U fuel cycle. *Nuclear Engineering and Design*, 263, 193–205. <https://doi.org/10.1016/j.nucengdes.2013.04.018>
9. Abdelghafar Galahom, A., Bashter, I. I., Aziz, M. (2015). Design of an MCNPX model to simulate the performance of BWRs using thorium as fuel and its validation with HELIOS code. *Annals of Nuclear Energy*, 77, 393–401. <https://doi.org/10.1016/j.anucene.2014.11.030>
10. Insulander Björk, K., Phager, V., Demazière, C. (2011). Comparison of thorium-based fuels with different fissile components in existing boiling water reactors. *Progress in Nuclear Energy*, 53 (6), 618–625. <https://doi.org/10.1016/j.pnucene.2010.03.004>
11. Carvalho, K. de A., Barros, G., Araujo, M. H. S., Vieira, T. A. S., Gonçalves, R. C., Silva, V., Santos, A. A. C. dos. (2025). Neutronic analysis and safety considerations in an innovative nuscale-like core merging thorium dioxide and reprocessed fuel. *Nuclear Engineering and Design*, 433, 113874. <https://doi.org/10.1016/j.nucengdes.2025.113874>
12. Lapanporo, B. P., Su'ud, Z., Mustari, A. P. A. (2024). Comparison of the neutronic properties of the (Th-<sup>233</sup>U)O<sub>2</sub>, (Th-<sup>233</sup>U)C, and (Th-<sup>233</sup>U)N fuels in small long-life PWR cores with 300, 400, and 500 MW<sub>th</sub> of power. *Nukleonika*, 69(1), 3–12. <https://doi.org/10.2478/nuka-2024-0001>
13. BWRX-300 General Description (2023). GE Hitachi Nuclear Energy. Available at: [https://www.gevernova.com/content/dam/gepower-new/global/en\\_US/images/gas-new-site/en/bwrx-300/005N9751\\_Rev\\_BWRX-300\\_General\\_Description.pdf](https://www.gevernova.com/content/dam/gepower-new/global/en_US/images/gas-new-site/en/bwrx-300/005N9751_Rev_BWRX-300_General_Description.pdf)
14. Lapanporo, B. P., Su'ud, Z., Mustari, A. P. A. (2024). Neutronic design of small modular longlife pressurized water reactor using thorium carbide fuel at a power level of 300–500 MW<sub>th</sub>. *Eastern-European Journal of Enterprise Technologies*, 1 (8 (127)), 18–27. <https://doi.org/10.15587/1729-4061.2024.290996>
15. Insulander Björk, K. (2013). A BWR fuel assembly design for efficient use of plutonium in thorium–plutonium fuel. *Progress in Nuclear Energy*, 65, 56–63. <https://doi.org/10.1016/j.pnucene.2013.01.010>